Parameter Identification and Model Validation of a Macroscopic Traffic Model

Elvira Thonhofer * **Martin Fuhrmann** * **Stefan Jakubek** *

* *TU Wien, Institute of Mechanics and Mechatronics, Getreidemarkt 9/E325, 1060 Vienna, Austria (email: {elvira.thonhofer, martin.fuhrmann, stefan.jakubek}@tuwien.ac.at).*

Abstract: Adaptive traffic control algorithms require an underlying traffic model. A suitable macroscopic traffic model has previously been developed by the authors. In this work the proposed method of parameter identification and the traffic model are validated with real live traffic data PeMS (Performance Measurement System) provided by the California Institute of Transportation. The proposed method of parameter identification utilizes a genetic algorithm (GA) where the difference between measurement data and simulation data are minimized. Parameter sensitivity and identifiability are investigated via the Fisher Information Matrix. The macroscopic traffic model based on the identified parameters is used to simulate traffic for a given time period at the test field. Results are presented and cross-validated with both the provided data of the PeMS data base and simulation results of the stochastic cell transmission model.

Keywords: Traffic model, Optimization, Parameter estimation, Sensitvity analysis, Validation

1. INTRODUCTION

Urban traffic demand is steadily increasing, causing economic losses due to increased travel time in addition to air and noise pollution. Consequently, traffic network optimization is a very active area of research. In order to derive and develop traffic network optimization algorithms, suitable traffic models are required. Existing traffic models can be classified into microscopic models, where vehicles are modeled individually, and macroscopic traffic models, where traffic is treated as a compressible fluid. A popular model among the macroscopic approaches is the cell transmission model (CTM), (Daganzo, 1993, 1995b) which has been adapted to accurately describe various nonlinear traffic phenomena that are observed in reality and extended to road networks, (Daganzo, 1995a). Modified CTM are successfully utilized to estimate congestion in real time in large highway networks by incorporating traffic sensor data, (Muñoz et al., 2003). Finally, and relevant for this work, the CTM is extended to a stochastic CTM (SCTM) Sumalee et al. (2011). This approach allows for stochastic variation of model parameters based on the variations observed in measurement data.

The model investigated in this work Thonhofer et al. (2014) follows the macroscopic approach based on the nonlinear transport equation with a flux term governed by the speed of the flow. A first order numerical scheme is utilized which uses an arbitrary fundamental diagram (FD), i. e. it does not require a convex, differentiable flux function. The model parameters, i. e. the parameters of the FD can be updated online via measurement data. Thereby, maximum flexibility in rapidly changing environmental conditions and traffic situations is granted. This is critical for traffic optimization strategies.

However, one aspect of the human driver-behavior is generally neglected in macroscopic traffic models. Drivers usually exhibit a responsible foresight,i. e. they react to density or velocity gradients ahead to a varying degree depending on visibility, current speed and other factors. Drivers will reduce their speed if a congestion is sufficiently close ahead (and visible) even if the traffic density in the close vicinity of the drivers is low. Likewise, a driver will accelerate from a traffic signal that just turned green into an empty road section ahead despite the traffic density behind the traffic signal being at a maximum and would therefore allow zero speed. In addition to the parameters of the arbitrary FD we introduce a model parameter that describes driver foresight.

In order to accurately estimate parameters the quality of the collected data is critical. Not only functionality of the sensor itself but also the range of data collected at a given location need to be considered. Data should be collected in such a way that they provide maximum information output and hence also optimum estimation accuracy. Utilizing the Fisher Information Matrix (FIM), which is a common tool in design-of-experiments Hametner et al. (2013); Goodwin and Payne (1977), optimum sensor placement for a range of realistic traffic situations can be determined at the planning stage. However, in real live applications sensor placement is often predetermined or limited by site geometry, financial means or regulations. We show that the FIM can be used to determine whether a parameter can be identified (reliably) from the measurement data provided. In this work measurement data is provided by PeMS [1] based on traffic sensors installed along the highway section.

[1] http://pems.dot.ca.gov/

This paper is organized as follows: The macroscopic traffic model is briefly discussed in Section 2, the concept of parameter identification is discussed in Section 3. In Section 4 both the parameter identification and the macroscopic traffic models are validated. Results are shown in Section 4.6. Finally, conclusive remarks are provided in Section 5.

2. MACROSCOPIC TRAFFIC MODEL

The traffic model under investigation in this work is presented briefly in Thonhofer et al. (2014) and in depth including network application, parameter identification and sensitivity analysis in Thonhofer et al. (2016 (in press) which is currently in press. Therefore, the model is introduced only in such detail as needed to follow the validation process. The interested reader is referred to the cited works for a detailed discussion.

The macroscopic traffic model is based on the transport equation, a hyperbolic partial differential equation

$$\frac{\partial \rho(x,t)}{\partial t} + \frac{\partial \phi(\rho(x,t))}{\partial x} = 0, \quad x \in \mathbb{R}, t \geq 0 \tag{1}$$

where ρ represents the vehicle density in [vehicles/m], x and t represent the spatial and temporal coordinate respectively, and $\phi(\rho(x,t))$ represents the (arbitrary) flux function

$$\phi(\rho, x, t) = f(\rho, x, t) = \rho(x,t) \cdot v(\rho), \quad \text{[vehicles/s]} \tag{2}$$

The shape of the flux function ϕ is governed by the relation between driving speed $v(\rho)$ and the local density ρ - the FD. In this work, we show that the parameters of the FD can be identified from measurement data, see section 4.4.

Additionally, we introduce a foresight coefficient α

$$\alpha = \alpha(\rho, x, t, \dots), \quad \alpha \in [0, 1) \tag{3}$$

which describes the extent to which a driver is forward-oriented in their driving behavior. In real life the amount of foresight depends on factors such as visibility and driver personality. Note, that α also depends on the spatial discretization length, since it is closely related to visibility of downwind road sections. As part of the numeric scheme we identify the value of α along with the parameters of the FD.

2.1 Discrete Cell Model

In order to solve (1) the spatial domain is discretized into cells along the length of a given road. Note that all lanes are lumped in a cell. In the scope of this work we assume that all cells use the same parameter vector $\boldsymbol{\theta}$. The vehicle (mass) balance for each cell i at a discrete time n is given by

$$\rho_i^{n+1} = \rho_i^n + (\phi_{i-1}^n - \phi_i^n)\frac{\Delta t}{\Delta x}, \quad i \in \mathcal{D}, n \geq 0 \tag{4}$$

where ϕ_{i-1}^n denotes the flux entering cell i, ϕ_i^n denotes the flux exiting cell i and $\mathcal{D}$ denotes the discrete spatial domain. The fraction $\frac{\Delta t}{\Delta x}$ accounts for temporal and spatial increments, respectively, that are restricted by the Courant-Friedrichs-Lewy (CFL) Condition for stability (Courant et al., 1967). The following constraints apply for density in any cell and all time steps:

$$0 \leq \rho_i \leq \rho_{\max} \tag{5}$$

Additional constraints such as flux limits can be imposed as well and must be observed in (6).

2.2 Boundary Conditions

Boundary Conditions (BC) are realized via ghost cells at every end of the computational domain. These cells are denoted ρ_0^n and ρ_{I+1}^n, respectively. The following BC are used in this work:

- absorbing BC: representation of an open domain outlet without reflection of information at the domain boundary
- inlet BC: given (measured) inflow or feed from preceding traffic light/crossing
- outlet BC: traffic light switches between absorbing BC (green light) and zero outflow (red light)

2.3 Numerical Scheme

The discretized mass balance given by (4) is sequentially solved, starting at the downwind end of $\mathcal{D}$, subject to BC and constraints given by (5). We compute the largest possible inflow ϕ_{i-1}^n into a given cell while observing constraints. At this point ϕ_I^n is known, because it is fully defined by the BC. For clarity, the equations are summarized

$$\max_{0 \leq c \leq 1} \phi_{i-1}^n = c \cdot \left(\rho_{i-1}^n v_{i-1}^n\right) \tag{6}$$

$$\text{s.t.} \quad \rho_i^{n+1} = \rho_i^n + (\phi_{i-1}^n - \phi_i^n)\frac{\Delta t}{\Delta x}, \quad i \in \mathcal{D}, n \geq 0$$

$$\rho_i \leq \rho_{\max}$$

$$\rho_i \geq 0$$

where $c \in [0, 1]$ is the flux limiting coefficient. Any method for solving the given optimization problem will suffice, however, in this particular case the solution can easily be found analytically. The inflow ϕ_{i-1}^n is defined by

$$\phi_{i-1}^n = f \cdot \rho_{i-1}^n v_{i-1}^n = f \cdot \rho_{i-1}^n((1-\alpha)v(\rho_{i-1}) + \alpha v(\rho_i)). \tag{7}$$

Then, one can rearrange the constraint equations and arrive at

$$f_i^n \leq \frac{(\rho_{\max} - \rho_i^n)\frac{\Delta x}{\Delta t} + \phi_i^n}{\rho_{i-1}^n v_{i-1}^n} = C \tag{8}$$

where C can be computed, because the BC for the cell with index I or the previously computed ϕ_{i-1}^n of the downwind cell is known. A time step is completed, once (8) is sequentially solved for every cell within $\mathcal{D}$.

3. PARAMETER IDENTIFICATION

We investigate how model parameters influence the model output over space and time and we present a methodology to identify the parameters of the FD based either only on one single or on multiple spatial traffic density observations. In addition, we propose a measure to assess in how far parameters of the FD are identifiable from given observations. For this purpose we utilize the Fisher information Matrix $\boldsymbol{\mathcal{I}}$, (Goodwin and Payne, 1977).

For a simple FD we define a parameterization as depicted in Fig. 1. The set of parameters that is used in the model is collected in a vector $\boldsymbol{\theta}$

$$\boldsymbol{\theta} = [\theta_1 \ \theta_2 \ \theta_3 \ \theta_4 \ \theta_5 \ \theta_6 \ \alpha] \tag{9}$$

where θ_i are the parameters defining the functional form of the FD and α is the foresight coefficient. The functional form of the FD is chosen as a piecewise linear

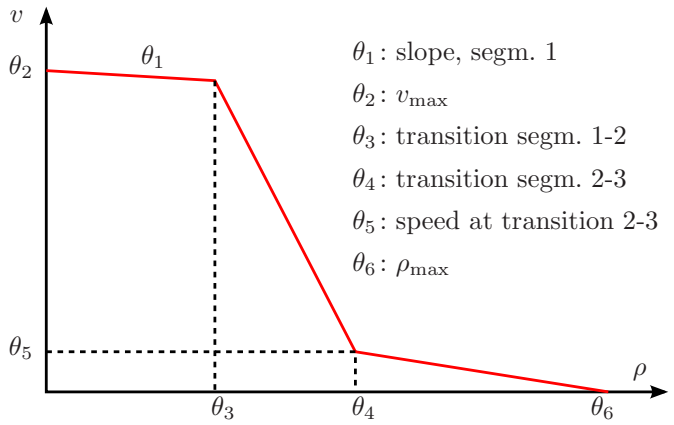

Fig. 1. Parameterization of a generic FD.

function. This particular choice is practical and supported by measurement data, see Section 4 for details. To avoid cluttering, all formulas are given with the assumption, that all cells within $\mathcal{D}$ observe the same parameter vector $\boldsymbol{\theta}$.

3.1 Parameter Sensitivity

Traffic sensors are placed at discrete points in the spatial domain. To acquire sufficient data we use the output error (OE) approach, which is based on past model outputs Hametner et al. (2013). The given updating scheme as defined by (4) results in a three-point stencil

$$\hat{\rho}_i^n = f(\hat{\rho}_{i-1}^{n-1}, \hat{\rho}_i^{n-1}, \hat{\rho}_{i+1}^{n-1}, \boldsymbol{\theta}) \tag{10}$$

where $\hat{\rho}_i^n$ represents a model output. The parameter sensitivity vector $\boldsymbol{\psi}_{i,\mathrm{OE}}^n$ is defined by the total derivative of the model output with respect to $\boldsymbol{\theta}$

$$\boldsymbol{\psi}_{i,\mathrm{OE}}^n = \frac{d\,\hat{\rho}_i^n(\boldsymbol{\theta})}{d\boldsymbol{\theta}} = \underbrace{\frac{\partial\,\hat{\rho}_i^n(\boldsymbol{\theta})}{\partial\boldsymbol{\theta}}}_{\boldsymbol{\psi}_{i,\mathrm{part}}^n} + \frac{\partial\,\hat{\rho}_i^n(\boldsymbol{\theta})}{\partial\,\boldsymbol{x}_i^n(\boldsymbol{\theta})} \left(\frac{d\,\boldsymbol{x}_i^n(\boldsymbol{\theta})}{d\boldsymbol{\theta}}\right)^T \tag{11}$$

with the regressor vector

$$\boldsymbol{x}_i^n(\boldsymbol{\theta}) = \left[\hat{\rho}_{i-1}^{n-1} \;\; \hat{\rho}_i^{n-1} \;\; \hat{\rho}_{i+1}^{n-1}\right]^T \tag{12}$$

containing the corresponding past model outputs. The term $\boldsymbol{\psi}_{i,\mathrm{part}}^n$ represents the partial derivative of the model output with respect to $\boldsymbol{\theta}$. Inserting (12) into (11) yields

$$\begin{aligned}\boldsymbol{\psi}_{i,\mathrm{OE}}^n &= \boldsymbol{\psi}_{i,\mathrm{part}}^n + \frac{\partial\,\hat{\rho}_i^n(\boldsymbol{\theta})}{\partial\,\boldsymbol{x}_i^n(\boldsymbol{\theta})} \left(\frac{d\left[\hat{\rho}_{i-1}^{n-1} \;\; \hat{\rho}_i^{n-1} \;\; \hat{\rho}_{i+1}^{n-1}\right]^T}{d\boldsymbol{\theta}}\right)^T \\ &= \boldsymbol{\psi}_{i,\mathrm{part}}^n + \frac{\partial\,\hat{\rho}_i^n(\boldsymbol{\theta})}{\partial\,\boldsymbol{x}_i^n(\boldsymbol{\theta})} \left[\boldsymbol{\psi}_{i-1,\mathrm{OE}}^{n-1} \;\; \boldsymbol{\psi}_{i,\mathrm{OE}}^{n-1} \;\; \boldsymbol{\psi}_{i+1,\mathrm{OE}}^{n-1}\right]^T.\end{aligned} \tag{13}$$

Fig. 2 illustrates the recursive scheme. The region of influence of $\boldsymbol{\theta}$ is bounded by the blue arrows, initial conditions and BC.

At time step $n = 0$ the solution is initialized with initial conditions, which do not depend on $\boldsymbol{\theta}$. Hence, the total derivative is defined

$$\text{for } n = 1: \quad \frac{d\,\hat{\rho}_i^{n-1}}{d\boldsymbol{\theta}} \stackrel{!}{=} 0, \quad \forall i \in \mathcal{D}. \tag{14}$$

Analogously, the total derivative at ghost cells with data inlet BC are defined

$$\frac{d\,\hat{\rho}_0^n}{d\boldsymbol{\theta}} \stackrel{!}{=} 0, \quad \text{if } \hat{\rho}_0^n = \rho_{\mathrm{data}}^n \tag{15}$$

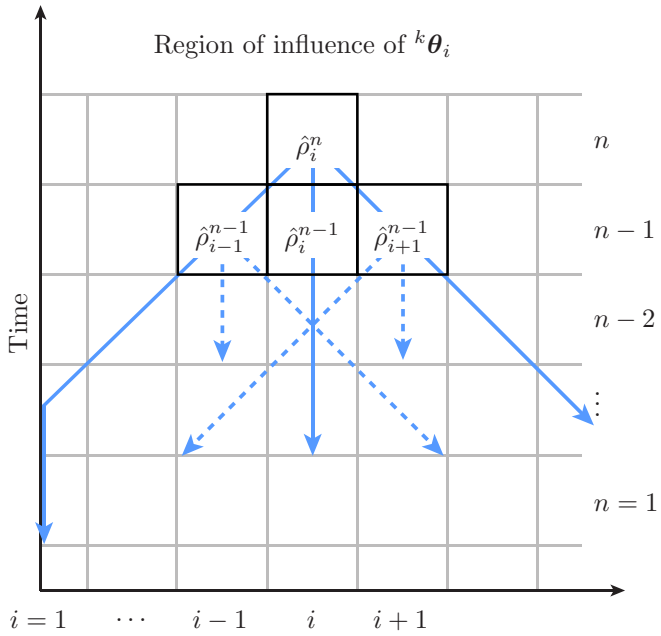

Fig. 2. Region of influence of $\boldsymbol{\theta}$ based on a three-point stencil.

3.2 Fisher Information Matrix

In the previous Section we assumed that all parameters influence the simulation result and, consequently, all parameters can be identified. However, identifiability is generally not guaranteed. There are two situations in which a parameter can not be identified:

- A parameter never affects the simulation result in any experiment setting.
- A parameter does not affect the simulation result in a particular setting.

In the first case the parameter should be dropped from the model entirely. The second case must be analyzed.

The conventional FIM $\boldsymbol{\mathcal{I}}$ is based on $\boldsymbol{\psi}_{i,\mathrm{part}}^n$, (Goodwin and Payne, 1977). However, we use the FIM $\boldsymbol{\mathcal{I}}_{\mathrm{OE}}$ in the output error (OE) configuration, (Hametner et al., 2013), which is based on $\boldsymbol{\psi}_{i,\mathrm{OE}}^n$. Thereby the dynamic influence of $\boldsymbol{\theta}$ on past model outputs is taken into account. It is defined by

$$\boldsymbol{\mathcal{I}}_{\mathrm{OE}} = \frac{1}{\sigma^2} \sum_{i,\,n} \underbrace{\left(\frac{d\,\hat{\rho}_i^n(\boldsymbol{\theta})}{d\boldsymbol{\theta}}\right)^T}_{\boldsymbol{\psi}_{i,\mathrm{OE}}^n} \left(\frac{d\,\hat{\rho}_i^n(\boldsymbol{\theta})}{d\boldsymbol{\theta}}\right) \tag{16}$$

where σ^2 is the variance of the estimated parameters. The FIM is essentially a square matrix describing the information content of a measurement data set based on the parameter sensitivity defined by (11).

We use a scalar criterion to evaluate the quality of the collected data set, i. e. it's information content with respect to the model parameters. Among the common criteria, (Goodwin and Payne, 1977), we choose the following criterion

$$J_S = \kappa_{\min}(\boldsymbol{\mathcal{I}}) \tag{17}$$

where the smallest singular value κ_i is maximized.

For the parameter identification itself we formulate an optimization problem. The *optimization goal* is to minimize

the error J_{OE}, see (18), computed by the *objective function* for the given system via variation of the *decision variables* $\boldsymbol{\theta}$ while observing *constraints* on $\boldsymbol{\theta}$. The model introduced in Section 2 with its BC and prescribed input values ρ_0 represents the *system* which acts as a constraint as well. The objective function evaluates the normalized output error defined by

$$J_{\mathrm{OE}} = \sum_{(j,s),\, n} \left\| \frac{(\hat{\rho}^n_{j,s} - \rho^n_{j,s})}{\max(\boldsymbol{\rho}_{j,s})} \right\|_2 \tag{18}$$

where

$$\boldsymbol{\rho}_{j,s} = \left[\rho^1_{j,s} \ \cdots \ \rho^n_{j,s}\right] \tag{19}$$

denotes the vector of collected measurement data at the sensor location (j, s) in the time interval $[0 \dots n]$. Essentially, the cost function captures the absolute difference between the simulation result and ground truth at each time step, summed up over all performed time steps n and all sensor locations (j, s).

4. VALIDATION OF CONCEPT

The real live traffic data used in this work is provided by the PeMS database. The test field and time frame are chosen in accordance with the test field and time frame used in the works of Sumalee et al. (2013) to allow for fair comparison of the traffic models.

4.1 Test Field

The test field is a section of Interstate 210 West between S Myrtle Ave through W. Huntington Dr to N Santa Anita Ave. The section is equipped with single loop inductance detectors which are embedded in the pavement along the mainline, HOV line and on- and off-ramps. We use accumulated data over all lanes for every 5-minute interval. The section is sketched in Fig. 3. Traffic data for the model validation is collected on April 22, 2008, 04:00 - 13:00. Additionally, data of the same section on April 29, 2008, 04:00 - 13:00 is utilized in the parameter identification.

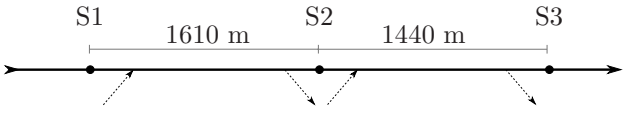

Fig. 3. Test site on I-210 West with sensors S1 (ID 761356), S2 (ID 761342) and S3 (ID 764146)

Data collected at sensor S1 is used as model input. Data from sensor S3 is used additionally in the identification of parameters. Data collected at sensor S2 serves as a checkpoint where simulation data is compared against ground-truth measurement data. Furthermore, it is assumed that traffic on on- and offramps is negligible. Simulation results suggest, that for this particular highway section the simplification does not introduce significant errors.

4.2 Data acquisition

Data provided by the PeMS database is directly applicable and does not require preprocessing in order to be used as model input. The PeMS database provides the following data:

The *occupancy* is a quantity which is measured by a detector. It is the percentage of time that a detector is on for a given time period. The *flow* $\boldsymbol{\phi}$ is a quantity measured by the loop detectors. The flow is reported in units of [vehicles/time]. The *speed* v is either measured directly via radar detectors or is calculated using a g-factor, the flow, and occupancy for single-loop detectors. Aggregated speed, that spans all of the lanes, is the flow-weighted mean across the lanes. The *g-factor* of a detector is listed for each detector. It is the effective vehicle length, in miles, for the detector.

Occupancy is used as a surrogate for the traffic density ρ in units of [vehicles/m] and is used directly as input for simulations. Initial conditions along the test field must be assumed, since sensor data along the length of the section is not available. However, very low traffic is expected at the time of initialization and the initial condition is set to zero without introducing noticeable errors.

PeMS data is accumulated for 5-minute intervals. Hence, in order to be applicable in the proposed model, intermediate data points are interpolated linearly, where needed.

4.3 Model of the test field

We consider all lanes lumped together into a virtual single lane road with a total length of 1.85 miles (3 km). We use a temporal discretization $\Delta t = 1$s, yielding 32100 time steps, and a spatial discretization of $\Delta x \approx 37$m, yielding 80 cells. The speed limit is unknown and irrelevant, since the model parameters are identified via measurement data collected by sensor S3. Note, that the temporal and spatial resolution are related via the CFL-condition, which in turn is governed by the maximum speed of the flow as estimated and given by θ_2.

Initially, the entire test field is assumed to be empty. The left boundary condition ρ^n_0 (inflow) is provided by the sensor S1.

4.4 Identification of model parameters

In an initial step plausibility of the provided measurement data is briefly investigated. The collected data points (density-speed couplets) of all three sensor locations (in color with different marker types) are depicted in Fig. 4. Additionally, the FD as identified by solving the optimization problem stated below is plotted in red.

For the given setup the optimization problem as described in Section 3 is formulated. The model parameters $\boldsymbol{\theta}$ are the decision variables. Initial conditions, BC and constraints are defined above. To accelerate the GA reasonable upper and lower bounds, UB and LB, respectively, for each model parameter are defined:

$$UB = [\quad 0 \ 35 \ 0.32 \ 0.52 \ 15 \ 1.2 \ 0.99]^T \tag{20}$$

$$LB = [-20 \ 15 \ 0.04 \ 0.12 \quad 1 \ 0.2 \ 0.10]^T \tag{21}$$

The GA is run with MATLAB® 2014b default settings (select method, elite count, crossover fraction, mutation rate), number of generations $g = 100$ and population $p = 70$ and yields a parameter vector

$$\boldsymbol{\theta}_{\mathrm{S3}} = [-2.7 \ 32.1 \ 0.09 \ 0.29 \ 10.7 \ 0.54 \ 0.87]^T \tag{22}$$

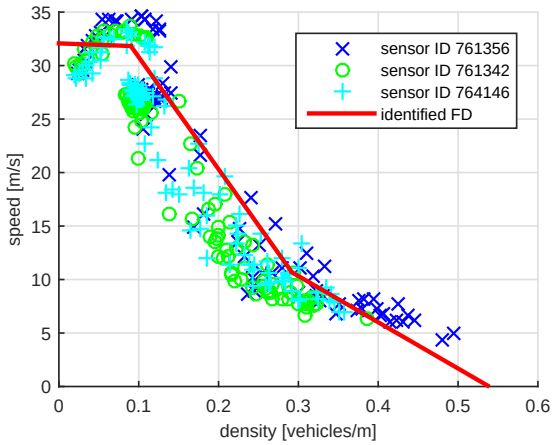

Fig. 4. Measurement data of three sensors (data points in color with different marker types) and the identified FD (red line)

where the subscript S3 indicates, that data from sensor S3 is used for identification. As a rule of thumb, the population size is chosen as $p \approx 10 \cdot n_{\text{parameters}} = 70$ to ensure a sufficiently diverse population that covers the entire input space well. The number of generations required for the GA depends on the problem and the initialization and is best kept conservatively large, to avoid premature termination of the optimization.

4.5 Parameter Sensitivity and Identifiability

As described in Section 3 identifiability of parameters is evaluated via the FIM, (16). The estimated variance of errors $\hat{\sigma}^2$ is defined by

$$\hat{\sigma}^2 = \frac{\text{SSE}}{\text{nt} - \text{np}}, \quad \text{with} \quad \text{SSE} = \sum_{(j,s),n} (\hat{\rho}^n_{j,s} - \rho^n_{j,s})^2 \tag{23}$$

where $\text{nt} = 32000$ is the number of considered time steps and $\text{np} = 7$ is the number of model parameters. Parameter sensitivity $\boldsymbol{\psi}^n_{i,\text{OE}}$ as defined by the recursive (13) is computed for cell $i = 80$ representing sensor S3 and all time steps.

The SVD of the FIM is computed and yields singular values σ_i collected in a vector $\boldsymbol{\Sigma}$

$$\boldsymbol{\Sigma} = [2.16e7 \;\; 3.01e3 \;\; 35.73 \;\; 1.85 \;\; 2.73\text{e-}2 \;\; 3.10\text{e-}3 \approx 0] \tag{24}$$

and the corresponding right-singular vectors $\boldsymbol{v_i}$ are collected in $\boldsymbol{V}^*$:

$$\boldsymbol{V}^* = \begin{bmatrix} \approx 0 & \approx 0 & \approx 0 & -0.99 & \approx 0 & \approx 0 & \approx 0 \\ \approx 0 & \approx 0 & -0.99 & \approx 0 & \approx 0 & \approx 0 & \approx 0 \\ \approx 0 & \approx 0 & \approx 0 & \approx 0 & \approx 0 & 0.99 & \approx 0 \\ \approx 0 & \approx 0 & \approx 0 & \approx 0 & \approx 0 & \approx 0 & 0.99 \\ \approx 0 & 0.48 & \approx 0 & \approx 0 & -0.88 & \approx 0 & \approx 0 \\ \approx 0 & 0.87 & \approx 0 & \approx 0 & 0.48 & \approx 0 & \approx 0 \\ -0.99 & \approx 0 & \approx 0 & \approx 0 & \approx 0 & \approx 0 & \approx 0 \end{bmatrix}. \tag{25}$$

Numbers are given with power-10 exponential notation, e. g. $1.2 \times 10^{-1} = 1.2\text{e-}1$. The right-singular vectors form an orthogonal basis in the parameter space. The singular value corresponding to a right-singular vector is a measure for the effect that a unit change along the direction of the vector has on the model output at the investigated sensor location. In this example $\sigma_7 \approx 0$, the corresponding $\boldsymbol{v_7}$ points along parameter θ_4. One can conclude that a small change in θ_4 is not noticeable in the measurement data collected at sensor S3. Note here, that we can not conclude that θ_4 can be dropped from the model entirely or that it is irrelevant for simulation results at any other location along the test field. However, the fact that the precise value θ_4 is of little importance is plausible, since it defines the transition point between section 2 and 3 in the FD, see Fig. 4, which is not particularly well defined by measurement data. Interestingly, the foresight coefficient α corresponds to σ_1, indicating that a slight change of α significantly influences the model output at the sensor location.

4.6 Simulation results

To verify the quality of the parameter identification and, inplicitly, the information content of the measurement data provided by the chosen sensor location, traffic simulations are performed. Results are compared against ground truth measurement data collected at S2 provided by the PeMS database. Figure 5 shows simulation results for April 22, 2008 which is solely used for *validation* of the traffic model and the process of parameter identification. The simulation results for April 29, 2008 are shown in

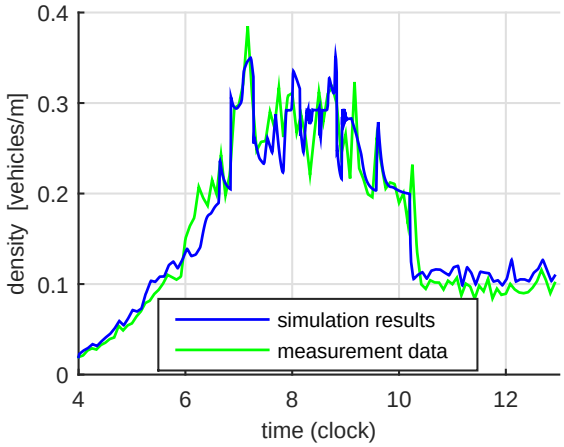

Fig. 5. Simulation results at sensor S2 (ID 761342) on April 22, 2008 (blue) and PeMS data for reference (green).

Fig. 6. Data collected on this day is used for parameter identification.

Finally, the computed density over space and time is shown in Fig. 7 and compared against ground truth data provided by the PeMS database shown in Fig. 8. It is obvious that the simulation results match the ground truth very well.

5. CONCLUSION AND OUTLOOK

We use measurement data provided by PeMS to estimate model parameters for a given section of I-210. Additionally, we utilize the FIM to gain insight as to which parameters are estimated reliably. Parameters that can not be estimated reliably must be used with caution, since they might be of significance in different experiment settings.

The method of parameter identification is validated by performing a simulation with the estimated parameters for

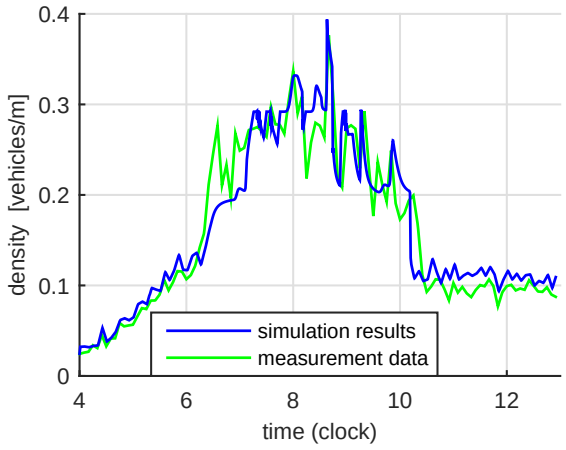

Fig. 6. Simulation results at sensor S2 (ID 761342) on April 29, 2008 (blue) and PeMS data for reference (green).

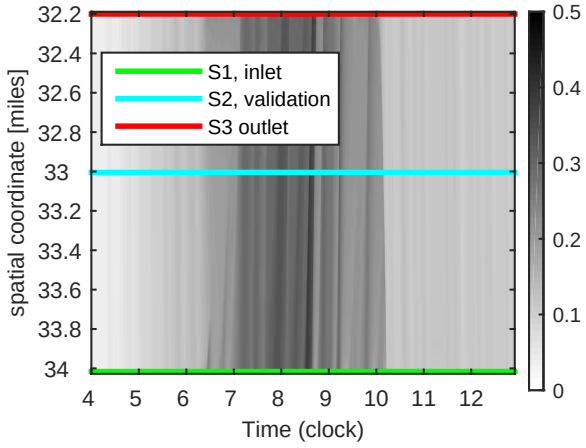

Fig. 7. Traffic density over the entire domain for April 22, 2008 as a simulation result.

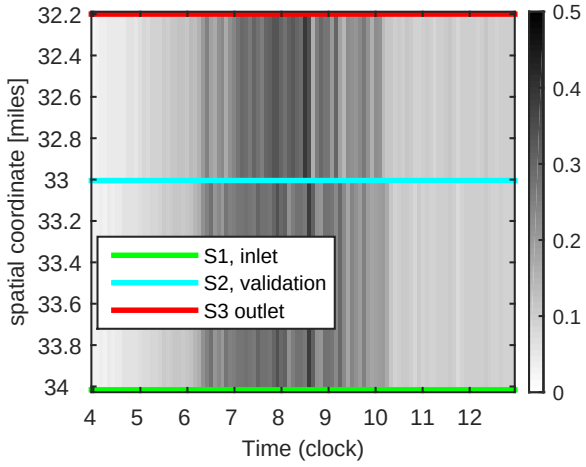

Fig. 8. Traffic density over the entire domain for April 22, 2008 as provided by PeMS.

a different day at the given section of I-240 and comparing simulation results with ground truth measurement data. Results show that the methods proposed in Thonhofer et al. (2016 (in press) perform very well with measurement data. Furthermore, results comply very well with the results published in Sumalee et al. (2011).

In the future the proposed model and methods will be validated for urban traffic scenarios.

ACKNOWLEDGEMENTS

This research was partially funded by Wirtschaftsagentur Wien (ID 1464714).

REFERENCES

Courant, R., Friedrichs, K., and Lewy, H. (1967). On the partial difference equations of mathematical physics. *IBM journal of Research and Development*, 11(2), 215–234.

Daganzo, C.F. (1993). The cell transmission model. part i: A simple dynamic representation of highway traffic. Technical report, Institute of Transportation Studies, University of California, Berkeley. doi:UCB-ITS-PRR-93-07.

Daganzo, C.F. (1995a). The cell transmission model, part ii: network traffic. *Transportation Research Part B: Methodological*, 29(2), 79–93.

Daganzo, C.F. (1995b). A finite difference approximation of the kinematic wave model of traffic flow. *Transportation Research Part B: Methodological*, 29(4), 261–276.

Goodwin, G.C. and Payne, R.L. (1977). Dynamic system identification: experiment design and data analysis.

Hametner, C., Stadlbauer, M., Deregnaucourt, M., Jakubek, S., and Winsel, T. (2013). Optimal experiment design based on local model networks and multilayer perceptron networks. *Engineering Applications of Artificial Intelligence*, 26(1), 251–261.

Muñoz, L., Sun, X., Horowitz, R., and Alvarez, L. (2003). Traffic density estimation with the cell transmission model. In *American Control Conference, 2003. Proceedings of the 2003*, volume 5, 3750–3755. IEEE.

Sumalee, A., Pan, T., Zhong, R., Uno, N., and Indra-Payoong, N. (2013). Dynamic stochastic journey time estimation and reliability analysis using stochastic cell transmission model: Algorithm and case studies. *Transportation Research Part C: Emerging Technologies*, 35, 263–285.

Sumalee, A., Zhong, R., Pan, T., and Szeto, W. (2011). Stochastic cell transmission model (sctm): a stochastic dynamic traffic model for traffic state surveillance and assignment. *Transportation Research Part B: Methodological*, 45(3), 507–533.

Thonhofer, E., Luchini, E., and Jakubek, S. (2016 (in press)). A flexible, adaptive traffic network simulation with parameter identification. *Journal of Intelligent Transportation Systems*.

Thonhofer, E., Luchini, E., Kuhn, A., and Jakubek, S. (2014). Online parameter estimation for a flexible, adaptive traffic network simulation. In *Connected Vehicles and Expo (ICCVE), 2014 International Conference on*, 937–938. IEEE.